ARTICLES

Analysis of pp-pp, πd-πd, and pp-πd processes concerning a narrow structure in pp-A_y data at $\sqrt{s} \sim 2.16$ GeV

J. Nagata and M. Matsuda
Division of Materials Science, Faculty of Integrated Arts and Sciences, Hiroshima University, Hiroshima 730, Japan

N. Hiroshige
Department of Applied Physics, Osaka City University, Osaka 558, Japan

T. Ueda
Faculty of Engineering Science, Osaka University, Osaka 560, Japan

(Received 24 June 1991)

A method is proposed for the analysis of pp-pp, πd-πd, and pp-πd processes concerning a narrow structure of KEK pp-A_y data ($\theta_c \approx 39°$) at $\sqrt{s} \simeq 2.16$ GeV. The analysis of these A_y data, together with the Saclay pp $d\sigma/d\Omega(\theta_c = 90°)$ data, indicates that the narrow structure can be explained by the structure of the $^3P_2$, $^3F_3$, or $^3H_5$ wave, while the structure in the $^3F_3$ or $^3H_5$ wave is more favorable than that in the $^3P_2$ wave. Furthermore, the analyses are extended to the other data on pp-pp, πd-πd, and pp-πd processes to restrict the solutions. Then the efficient observables for this purpose are proposed.

PACS number(s): 21.30.+y, 13.75.Cs, 13.75.Gx, 14.20.Pt

I. INTRODUCTION

The experimental data on the proton-proton total cross-section difference in the longitudinal spin states $\Delta\sigma_L = \sigma^{\text{tot}}(\rightleftarrows) - \sigma^{\text{tot}}(\rightrightarrows)$ have shown striking structures of the energy dependence with a width of about 100 MeV at $P_L = 1.26$ and 1.40 GeV/c [1]. These structures were shown to stem from the $^1D_2$ (2.17 GeV) and $^3F_3$ (2.22 GeV) waves on the basis of the phase-shift analysis of the elastic proton-proton scattering data in this energy region [2]. It has been shown that these structures are due to the πNN resonances by the three-body calculation of the πNN system [3].

Recently, narrow structures with a width of about 10 MeV have been observed in the data on the N-N system. They appear at $\sqrt{s} = 2.16$ and 2.19 GeV in the X-mass spectra of the ^{3}He$(p,d)X$ reaction [4(a)], and in the energy dependences of the analyzing power (A_y) data on the ^{3}He$(p,d)X$ reaction [4(b)] and the A_y data on elastic proton-proton scattering [5]. We need to investigate whether these narrow structures are concerned with the existence of dibaryons or not. No usual theory explains such a narrow structure. So we may expect that this problem is important to hadron-quark physics. The following problems must be examined: (1) Are the narrow structures in the energy dependence of A_y data on elastic p-p scattering [5] consistent with the data on other kinds of observables? (2) If consistent, which partial wave generates the narrow structure of the A_y data?

In Sec. II, a method of analysis of a narrow structure in observables is proposed. In Sec. III, we report the result of analysis of the p-p scattering data and, in Sec. IV, the results of analysis of the data on elastic π-d scattering and pp-πd reaction. Section V is devoted to some concluding remarks.

II. METHODS OF ANALYSIS

The analyzing power (A_y) of elastic p-p scattering at an angle of roughly 39° in the center-of-mass system (c.m.s.) has been measured at intervals of about 4 MeV and with an extreme accuracy (10% of the old data errors) in the energy region $T_L = 500$–920 MeV at Kou-Energy-Kenkyusho (KEK) [5]. The experimental data on more than nine kinds of observables at one energy point are needed to obtain a unique solution in the phase-shift analysis (PSA). But no data on so many kinds of observables are available except the A_y at some energy points in this energy region, and it is impossible to determine the partial-wave amplitudes by the PSA at present. In order to determine which partial waves participate in the narrow structures of the KEK A_y data, we propose the following method for analyzing elastic p-p scattering, π-d scattering and pp-πd reaction simultaneously.

(I) We assume that one narrow-structure is caused by one particular partial wave.

(II) We define the S matrix of the total angular momentum J and the parity P, which is assumed to produce the narrow structure of A_y as follows:

$$S^{ij}_{JP} = \delta^{ij} + 2i A^{ij}_{JP} , \tag{1}$$

where i and j denote the channels of pp or πd. The partial-wave amplitude A^{ij}_{JP} is divided into two terms as

$$A^{ij}_{JP} = B^{ij}_{JP} + R^{ij}_{JP} , \tag{2}$$

where B^{ij}_{JP} and R^{ij}_{JP} are respectively the background term and the narrow structure term. B^{ij}_{JP} for $i = j$ case is defined by

$$B^{ii}_{JP} = \frac{1}{2i}(\eta^i_{JP} e^{2i\delta^i_{JP}} - 1) , \tag{3}$$

and B^{ij}_{JP} for $i \neq j$ case is described in Sec. IV B, while the narrow structure term is parametrized by the resonance formula:

$$R^{ij}_{JP} = \frac{1}{2}\sqrt{\eta^i_{JP}}\sqrt{\eta^j_{JP}}e^{i(\delta^i_{JP}+\delta^j_{JP})} \times \frac{\sqrt{\Gamma^i}\sqrt{\Gamma^j}}{-\sqrt{s}+\sqrt{s_R}-(i/2)\Gamma_t} c(\sqrt{s}) . \quad (4)$$

Here δ^i_{JP} and η^i_{JP} are respectively the phase shift and the reflection parameter of channel i, and their energy dependences are smoothed as explained below. $c(\sqrt{s})$ is the factor for decreasing rapidly the effect of the resonance term at higher energies than the resonance energy [6]. $\sqrt{s_R}$, Γ_t, and Γ^i are the invariant mass, the total width, and the partial width of the assumed resonance in channel i, respectively, and Γ^i is parametrized as follows [6]:

$$\Gamma^i(k_i) = \gamma_i f_i(k_i/k_R) \quad (5)$$

and

$$f_i(x) = \frac{11x^{2l_i+1}}{1+10x^{2l_i+1}} , \quad (6)$$

where k_i and l_i are the momentum in c.m.s. and the orbital angular momentum on channel i, respectively, and k_R the resonance momentum. γ_i is a constant parameter. The cutoff factor is given by [6]

$$c(\sqrt{s}) = \exp\left[\frac{-(\sqrt{s}-\sqrt{s_0})^4}{(\sqrt{s_c}-\sqrt{s_0})^4}\right] , \quad (7)$$

where $\sqrt{s_0}$ is the pion-production threshold energy, $2m_N+m_\pi$, and s_c a fitted parameter larger than s_R for cutting off the resonance effect.

Such a parametrization of the R_{JP} term in the distorted-wave Born approximation (DWBA) could be considered to be a good approximation, if the narrow structure in the A_y data is caused by the physics at the short distances ($r \lesssim 1$ fm) and the background is determined by the physics in the peripheral region ($r > 1$ fm). In this case, we may ignore the relative phase between the resonance and background terms. However, generally, we could have the freedom of the relative phase. The relative phase factor is discussed later.

Equations (1)–(4) are the ones for the spin-uncoupled case. For pp and πd scattering, the parametrization of partial-wave amplitude for the spin-coupled case is as follows. For orbital angular momentum $l = J \pm 1$, the partial-wave amplitudes are given by

$$A_{JP} = \begin{bmatrix} B_{J,J-1}+R_{J,J-1} & B^J \\ B^J & B_{J,J+1}+R_{J,J+1} \end{bmatrix} , \quad (2a)$$

where $B_{J,J\pm1}$ and $R_{J,J\pm1}$ are respectively the background terms and the narrow structure terms with orbital angular momentum $l = J \pm 1$. We use the following parametrization for the background terms:

$$B_{J,J\pm1} = \frac{1}{2i}[(1-\rho_J^2)^{1/2}\eta_\pm \exp(2i\delta_\pm) - 1] \quad (3a)$$

and

$$B^J = \frac{1}{2}\rho_J\sqrt{\eta_+}\sqrt{\eta_-}\exp(i\delta_- + i\delta_+) , \quad (3b)$$

where $\delta_\pm$ and $\eta_\pm$ are the phase shifts and the reflection parameters with $l = J \pm 1$, respectively, and ρ_J is a complex parameter of the wave coupling. The terms $R_{J,J\pm1}$ are given as follows:

$$R_{J,J\pm1} = \frac{1}{2}\eta_\pm e^{2i\delta_\pm}\frac{\Gamma_1}{-\sqrt{s}+\sqrt{s_R}-(i/2)\Gamma_t} c(\sqrt{s}) , \quad (4a)$$

where Γ_i is the partial width of the resonance in pp or πd channel. In Eqs. (3a) and (3b), and (4a), the suffix P is understood in B, R, ρ, δ, or η.

In pp-πd reaction, the partial-wave amplitude for the spin-coupled case is as follows:

$$A_{JP} = \begin{bmatrix} B_{J,J-1}+R_{J,J-1} \\ B_{J,J+1} \end{bmatrix} , \quad (2b)$$

where $R_{J,J-1}$ and $B_{J,J\pm1}$ are described in Sec. IV B.

(iii) The background terms B_{JP}, $B_{J,J\pm1}$, and B^J are derived in a structureless form by the PSA for respective processes whose details are described in Secs. III and IV.

(iv) We determine the parameters of the narrow structure term so that they may fit the KEK A_y data. In the calculation, the narrow structure is generated in A_y from the interference between the resonance and background terms. Then the interference patterns vary depending on the state assigned to the resonance. Therefore, the information on the partial waves causing the narrow structure can be obtained from the interference pattern.

(v) By applying procedures (i)–(iv) not only to the p-p scattering, but also to the π-d scattering and the pp-πd reaction, the possible partial waves participating in the narrow structures are more stringently selected.

III. ANALYSIS OF p-p SCATTERING

Using the method described in the above section, we analyze the narrow structure at $T_L = 604$ MeV ($\sqrt{s} = 2.16$ GeV) in the energy dependence on the KEK A_y data on elastic p-p scattering at an angle of roughly 39° in the c.m.s. [5]. We are concerned primarily with this structure, since this is most pronounced with four standard deviations.

The PSA of the elastic p-p scattering data were performed in the kinetic energy region of the incident proton $T_L = 500$–716 MeV, so that the background terms were estimated. Firstly, by smoothing the energy dependence of all of the experimental data of each observable with spline-function method, we make the pseudodata which have no structures with a width less than 10 MeV. Secondly, we perform the PSA of these pseudodata to determine the partial-wave amplitudes which are the background terms. The numbers of the experimental data and the pseudodata used in the PSA and the χ^2 value at each energy are listed in Table I. At some ener-

TABLE I. The observables and their numbers of experimental data and pseudodata on elastic p-p scattering used in the phase-shift analysis (PSA) for determining the background term. The χ^2 values of the PSA solutions are also shown: $\chi^2=\sum_i[(\theta_i^{\rm th}-\theta_i^{\rm exp})/\Delta\theta_i]^2$, where $\theta_i^{\rm th}$ and $\theta_i^{\rm exp}$ are the calculated and experimental values of observables i, respectively, and $\Delta\theta_i$ the experimental error.

	Number of the used data							
T_L (MeV)	$d\sigma/dt$	A_y	A_{LL}	A_{NN}	Forward data	Others	Total number of data	χ^2 value
500	124	83	4	18	7	87	323	480
530	54	13	13	12	7		99	64
550	54	13	13	12	7		99	61
567	54	13	14	12	7		100	59
583	51	13	11	12	7		94	68
593	54	13	14	12	7		100	81
604	54	13	14	12	7		100	84
622	54	13	14	12	7		100	79
634	54	13	14	12	7		100	83
648	49	13	14	12	7		95	92
669	54	13	14	12	7		100	90
684	54	13	14	13	7		100	101
699	47	13	14	12	7		93	61
716	54	13	14	13	7		100	107

gy points in the small scattering-angle region, there are no data on the A_y and the spin-correlation parameter A_{SL}. Then their pseudodata for the PSA are obtained by interpolation of the experimental data at the other energies with the spline-function method. In the PSAs the scattering amplitudes of the partial waves with the orbital angular momentum $l\geq 6$ are given by the one-pion exchange. We calculate A_y in all cases where the narrow structure term is assigned to a state with total angular momentum $J\leq 5$ in the N-N system. As a result, we find that the structure of the $^3P_1$, $^3P_2$, $^3F_3$, $^1G_4$, or $^3H_5$ state can reproduce the KEK A_y data, as is seen in Fig. 1. The structure parameters obtained by best fitting to the KEK A_y data are given in Table II.

On the other hand, the differential cross section for elastic p-p scattering at $\theta_c=90°$ has been measured with extremely high accuracy at Saclay [7]. In Fig. 2, our results calculated by using the structure parameters in Table II are compared with the Saclay data. We find that the fits to the Saclay data are good in the $^3F_3$ and $^5H_5$ structure cases. But the fit is worse in the $^3P_2$ case although this fit is allowable. The result for $^3P_1$ case shows an apparent disagreement with the Saclay data at $T_L=580$–630 MeV, and the result for $^1G_4$ case is much worse, which is not shown. Thus the $^3P_1$ and $^1G_4$ cases are excluded. See the χ^2 values for the fits in Table II, where $\chi^2=\sum_i[(\theta_i^{\rm th}-\theta_i^{\rm exp})/\Delta\theta_i]^2$ with the calculated value $\theta_i^{\rm th}$ of observable i, its experimental value $\theta_i^{\rm exp}$, and experimental error $\Delta\theta_i$.

The possibility of diproton in the $^1S_0$ state is pointed out in the rotation model [4(a)]. In the $^1S_0$ case, the narrow peak in the A_y cannot be reproduced within the framework of the relative phase=0 as is in Eq. (4). When we remove the condition of the vanishing relative phase, we find that the peak is reproducible with the phase $\sim 225°$. In this case, however, the prediction of the $d\sigma/d\Omega(90°)$ deviates strongly from the data. Thus the $^1S_0$ assignment is not likely.

In Fig. 3, the energy dependence of the old data $d\sigma/d\Omega$ at $\theta_c\approx 40°$, whose references are given in Table III, is shown together with our calculated values. The shown data also have a dip structure at about $T_L=600$–650 MeV as is seen in the figure, which cannot be reproduced by our calculation in any case of the $^3P_2$, $^3F_3$, or $^3H_5$ structure. In order to reproduce this structure by our calculation, we need the elasticity x much

TABLE II. The resonance parameters of the obtained solutions, and the χ^2 values.

Mass (MeV)	Width (MeV)	Elasticity Γ_{pp}/Γ_t	Spin-parity	χ^2 value A_y 29 data	χ^2 value $d\sigma/d\Omega$ ($\theta_c=90°$) 30 data	Total
2161	10	0.18	$^3P_1$	22	477	499
2165	10	0.08	$^3P_2$	35	297	332
2160	10	0.14	$^3F_3$	21	54	75
2158	10	0.06	$^3H_5$	36	46	82

larger than that given in Table II. Such a large elasticity is inconsistent with the values obtained from the $d\sigma/d\Omega(\theta_c=90°)$ data [7] which have a smooth energy dependence. There might, however, be a possibility that the experimental normalization of the data at $T_L=500.7$ and 592.9 MeV is questionable, since these data given by the same group are shifted by the same amount from the background.

Furthermore, it is found that the measurements of the forward observables (σ_t, $\Delta\sigma_L$, and $\Delta\sigma_T$) at a small energy interval are useful to discriminate between these structure candidates, as is seen in Fig. 4. The references of the data are given in Table III.

The estimated background of *p-p* total cross-section fits to the data of Ref. DZ(55). The datum at $\sqrt{s}=2.153$ GeV on the narrow-structure lines of $^3F_3$ and $^3H_5$ is the one measured in KEK [Ref. YA(81)]. The three data measured by Yamamoto *et al.* [Ref. YA(81)] are printed

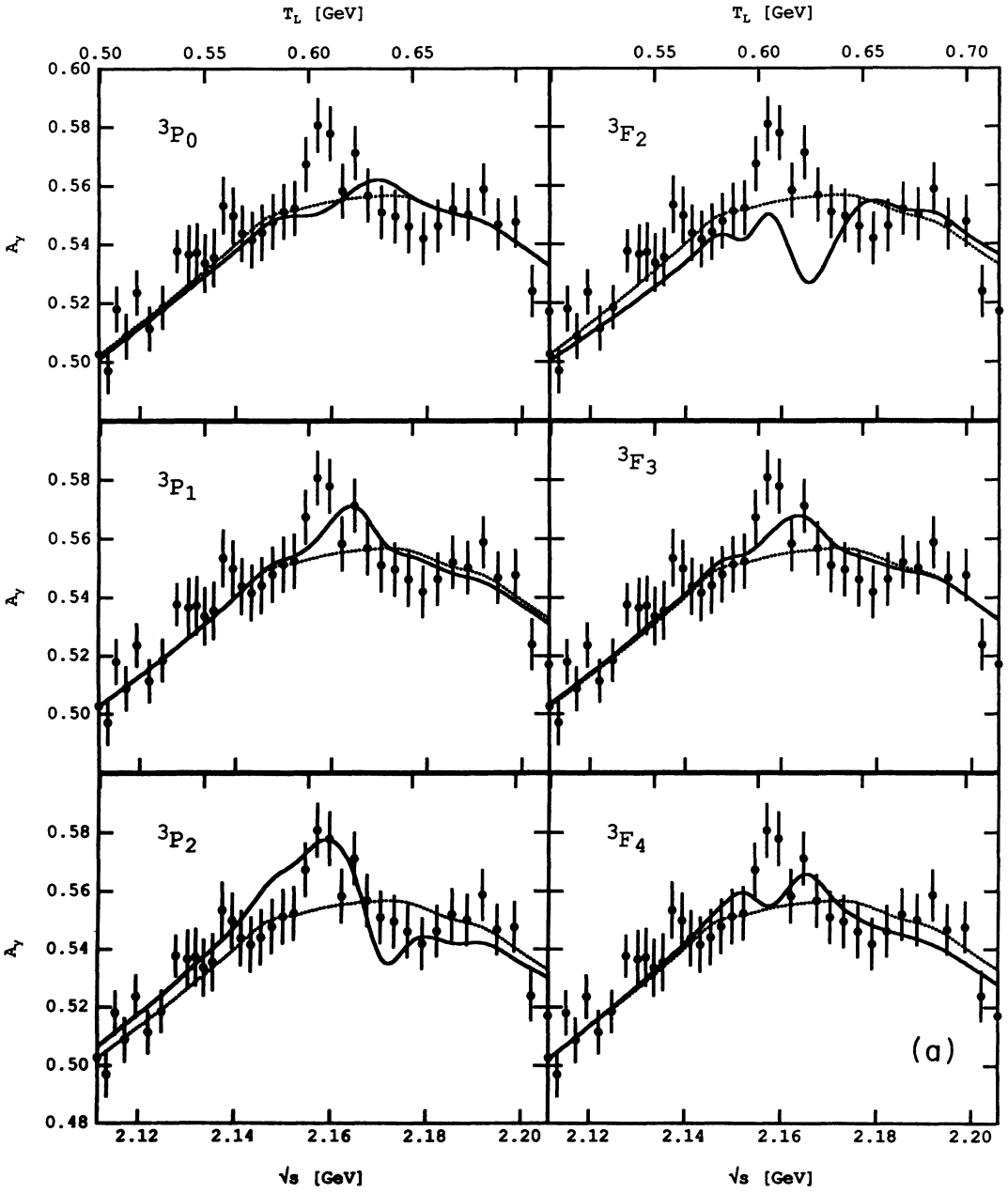

FIG. 1. The analyzing power A_y in *p-p* scattering calculated with the resonance amplitude $R_{JP}(J\leq 5)$ is shown by the dotted line, and their background value shown by the solid line. The resonance parameters are commonly taken as $\sqrt{s_R}=2165$ MeV, $\Gamma_t=10.0$ MeV, and $x=\Gamma_{pp}/\Gamma_t=0.08$. The experimental data are given by H. Shimizu *et al.* [5].

in Fig. 4(a), whose energies are $\sqrt{s}=2.115$, 2.153, and 2.188 GeV, respectively. The two data at lower energies are deviated from the background by the same extent, which might be due to the normalization different from that for the other data, but the datum at $\sqrt{s}=2.188$ GeV is on the background.

The data on p-p total cross section σ_t^{pp} seem to not support a resonant behavior at first glance. We remark the following about the data. The two Dubna data [DZ(55)] at $\sqrt{s}=2.15$ and 2.16 GeV are relatively accurate, fit the calculated background, and are not in support of the resonant behavior. However, this statement would be premature, if we observe that the KEK data [YA(81)] at 2.15 GeV have a tendency contradictory to the data of Dubna at 2.15 GeV. Therefore, we need accurate data on σ_t just at and surrounding the peak position for a definite conclusion.

The forward observables $\Delta\sigma_L$ and $\Delta\sigma_T$ also exhibit different energy dependence among these survived states as seen in Fig. 4. It is necessary to measure these observables in the region $T_L=550$–700 MeV. As for the dip structure of the energy dependence in the old experimental data, more accurate measurement of the $d\sigma/d\Omega$ at $\theta_c=40°$ is desired.

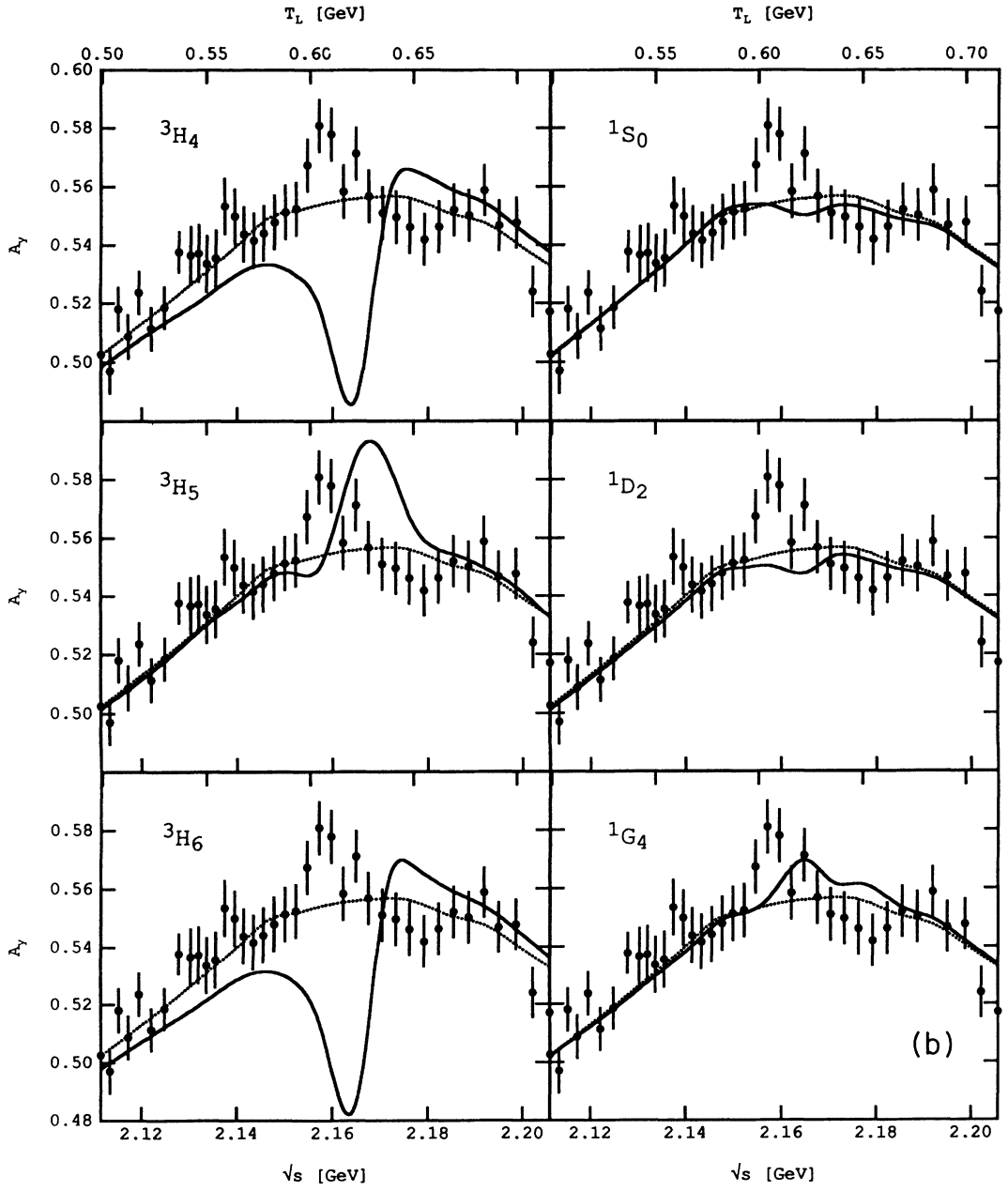

FIG. 1. (*Continued*).

TABLE III. The list of the experimental data on *p-p* scattering in Figs. 3 and 4, on π-*d* scattering in Fig. 5, and on *pp*-πd reaction in Fig. 6.

Observable	Number	References
Elastic *p-p* scattering		
$d\sigma/d\Omega(40°)$	7	AB(75),AL(70),BO(54),BO(72) GU(65),NI(65),RY(71)
σ_t	18	BU(66),CH(56),DZ(55),EL(59), GU(64),SC(71),YA(81)
$\Delta\sigma_L$	25	AP(84)1, AU(77),AU(81),AU(84), BY(84),ST(83)
$\Delta\sigma_T$	22	BI(78),DI(83),MA(85),PE(86), ST(83)
Elastic π-*d* scattering		
$d\sigma/d\Omega(117°)$	13	AK(83),BA(83),ST(80),GA(80)
$iT_{11}(117°)$	6	BO(81),OT(88),SM(84)
pp-πd reaction		
$d\sigma/d\Omega(117°)$	15	AL(71),BO(82),HO(84)1,MA(83), RI(70)
$A_{y0}(117°)$	16	AP(82),AP(84)2,HO(84)2, SA(83), TI(83)
$d\sigma/d\Omega(104°)$	8	AL(71),BA(62),NO(71),RI(70),RI(83)
$A_{y0}(104°)$	33	AL(71),AP(82),AP(84),CO(83), HO(83),TI(83),YO(90)

AB(75) K. Abe *et al.*, Phys. Rev. D **12**, 1 (1975).
AK(83) N. Akemoto *et al.*, Phys. Rev. Lett. **50**, 400 (1983).
AL(70) M. G. Albrow *et al.*, Nucl. Phys. **B23**, 445 (1970).
AL(71) M. G. Alblow *et al.*, Phys. Lett. **34B**, 337 (1971).
AP(82) E. Aprile *et al.*, Nucl. Phys. **A379**, 369 (1982).
AP(84)1 E. Aprile *et al.*, Nucl. Phys. **A431**, 637 (1984).
AP(84)2 E. Aprile *et al.*, Nucl. Phys. **A415**, 365 (1984).
AU(77) I. P. Auer *et al.*, Nucl. Phys. **67B**, 113 (1977).
AU(81) I. P. Auer *et al.*, Phys. Rev. D **24**, 2008 (1981).
AU(84) I. P. Auer *et al.*, Phys. Rev. D **29**, 2435 (1984).
BA(62) B. Baldoni *et al.*, Nuovo Cimento **26**, 1376 (1962).
BA(83) B. Balestri *et al.*, Nucl. Phys. **A392**, 217 (1983).
BI(78) Ed. K. Biegert *et al.*, Phys. Lett. **73B**, 235 (1978).
BO(54) N. P. Boghachev *et al.*, Dok Akad. Nauk. SSSR **99**, 931 (1954).
BO(72) E. T. Boschitz *et al.*, Phys. Rev. C **6**, 457 (1972).
BO(81) J. Bolger *et al.*, Phys. Rev. Lett. **46**, 167 (1981).
BO(82) J. Boswell *et al.*, Phys. Rev. C **25**, 2540 (1982).
BU(66) D. V. Bugg *et al.*, Phys. Rev. **146**, 980 (1966).
BY(84) J. Bystricky *et al.*, Phys. Lett. **142B**, 130 (1984).
CH(56) F. F. Chen *et al.*, Phys. Rev. **103**, 211 (1956).
CO(83) M. D. Corcoran *et al.*, Phys. Lett. **120B**, 309 (1983).
DI(83) W. R. Digzler *et al.*, Phys. Rev. D **27**, 680 (1983).
DZ(55) V. P. Dzhelepov *et al.*, SSSR **104**, 380 (1955).
EL(59) T. Elioff *et al.*, Phys. Rev. Lett. **3**, 285 (1959).
GA(80) K. Gabathuler *et al.*, Nucl. Phys. **A350**, 253 (1980).
GU(64) V. M. Guzhavin *et al.*, Zh. Eksp. Teor. Fiz. **46**, 1245 (1964) [Sov. Phys. JETP **19**, 847 (1964)].
GU(65) V. M. Gughavin *et al.*, Zh. Eksp. Teor. Fiz. **47**, 1228 (1964) [Sov. Phys. JETP **20**, 830 (1965)].
HO(83) J. Hoftiezer *et al.*, Phys. Rev. Lett. **51**, 759 (1983).
HO(84)1 J. Hoftiezer *et al.*, Nucl. Phys. **A412**, 286 (1984).
HO(84)2 J. Hoftiezer *et al.*, Nucl. Phys. **A402**, 429 (1984).
MA(83) E. L. Mathie *et al.*, Nucl. Phys. **A397**, 469 (1983).
MA(85) W. P. Madigan *et al.*, Phys. Rev. D **31**, 966 (1985).
NI(65) S. J. Nikitin *et al.*, Nuovo Cimento, **2**, 830 (1965).
NO(71) J. H. Norm, Nucl. Phys. **B33**, 512 (1971).

TABLE III. (*Continued*).

OT(88) C. R. Ottermann *et al.*, Phys. Rev. C **38**, 2310 (1988).
PE(86) F. Perrot *et al.*, Nucl. Phys. **B278**, 881 (1986).
RI(70) C. Richard-Serre *et al.*, Nucl. Phys. **B20**, 413 (1970).
RI(83) B. G. Ritchie *et al.*, Phys. Rev. C **27**, 1685 (1983).
RY(71) B. A. Ryan *et al.*, Phys. Rev. D **3**, 1 (1971).
SA(83) A. Saha *et al.*, Phys. Rev. Lett. **51**, 759 (1983).
SC(71) P. Schwaller *et al.*, Phys. Lett. **35B**, 243 (1971).
SM(84) G. R. Smith *et al.*, Phys. Rev. C **29**, 2206 (1984).
ST(80) A. Stanovnik *et al.*, Phys. Lett. **94B**, 323 (1980).
ST(83) S. P. Stanley *et al.*, Nucl. Phys. **A403**, 525 (1983).
TI(83) W. B. Tippens *et al.*, Xth International Conference on Few Body Problems in Physics, Karlsruhe, 1983 and private communication.
YA(81) S. S. Yamamoto *et al.*, Report KEK-EPC **80-01**, 1981.
YO(91) H. Yoshida, KEK Report No. 91-146.

In this analysis, the correct determination of the background term, which is maintained by the stability of the solution of PSA, is important. To accomplish this purpose, one should provide the accurate experimental data of the differential cross section and the analyzing power at small scattering angles: $\theta_c \lesssim 30°$.

IV. ANALYSIS OF DATA ON OTHER CHANNELS

A. π-d Elastic scattering

In order to study the effects of the narrow structure on the π-d elastic channel, we require a smooth background term similar to that of the p-p elastic case. In π-d scattering, it will be preferable to perform an energy-dependent PSA assuming analytical forms for scattering amplitudes, since the experimental data for the π-d elastic scattering, unlike the p-p elastic scattering, are not enough in quantity and quality at present.

On the other hand, three-body calculations based on the Faddeev equation are consistent with the experimental data in a gross feature. Thus it will be reasonable to start with these theoretical values. In the present analysis we make a modified energy-dependent PSA of the available data in the pion kinetic energy region $T_L = 65-325$ MeV using the Lyon group amplitudes of the Faddeev theory.[1,2]

For the η's and δ's of the s, p, and d waves, where we use the little character for the orbital angular momentum in πd channel, their energy dependences are simulated by polynomial expansions in the laboratory kinetic energy T_L

$$\delta = \sum_{n=0}^{4} a_n T_L^n , \tag{8}$$

$$\eta = \sum_{n=0}^{4} b_n T_L^n , \tag{9}$$

where a's and b's are floating parameters and their values are determined by the conventional χ^2-minimization procedure. The higher partial-wave amplitudes with the orbital angular momentum $3 \le l \le 8$ are fixed to the smooth Lyon ones [8] and those with $l \ge 9$ are neglected.

The starting values of the a's and b's are obtained by the least square fit to the Lyon amplitudes. They are calculated at 11 energy points among 13 points where the experimental data are available in the energy region considered here. The scattering amplitudes at the two remaining energy points are given by the interpolation with the spline function.

The Lyon amplitudes in the $^3p_2$ state, however, have rapid energy variation around $T_L = 180$ MeV and cannot be well reproduced by the mild forms of Eqs. (8) and (9). As a result, a solution with a satisfactory fit to the experimental data does not seem to be obtained. Therefore, we assume for the $^3p_2$ state the resonancelike form

$$\delta(^3p_2) = \frac{(a_4 - T_L)\sum_{n=0}^{3} a_n T_L^n}{(a_5 - T_L)^2 + a_6^2} , \tag{8a}$$

[1]A single-energy PSA has been attempted by several authors starting from Faddeev amplitudes or by constraining around these amplitudes [9,10].

[2]If we assume that the π-d elastic scattering and the related reactions are saturated by a three channel ($pp, \pi d, N\Delta$), then the moduli of the scattering amplitudes in the $^3p_2$ and $^3d_3$ states are constrained by the three-channel unitarity [9]. In the present analysis, we make a free search without this restriction on the scattering amplitudes.

$$\eta(^3p_2)=\frac{\sum_{n=0}^{4} b_n T_L^n}{(b_5-T_L)^2+b_6^2} . \tag{9a}$$

Using these parametrizations for the scattering amplitudes, we made a χ^2-minimization search and obtained a solution which reproduces well the experimental data. The numbers of the experimental data used in the PSA and the χ^2 values of the solution are listed in Table IV.

Taking the present PSA solution as the background terms [Eq. (3)], we calculate the energy dependence of $d\sigma/d\Omega$ and iT_{11} at $\theta_c=117°$ admixing the $^3d_3$ or $^3g_5$ res-

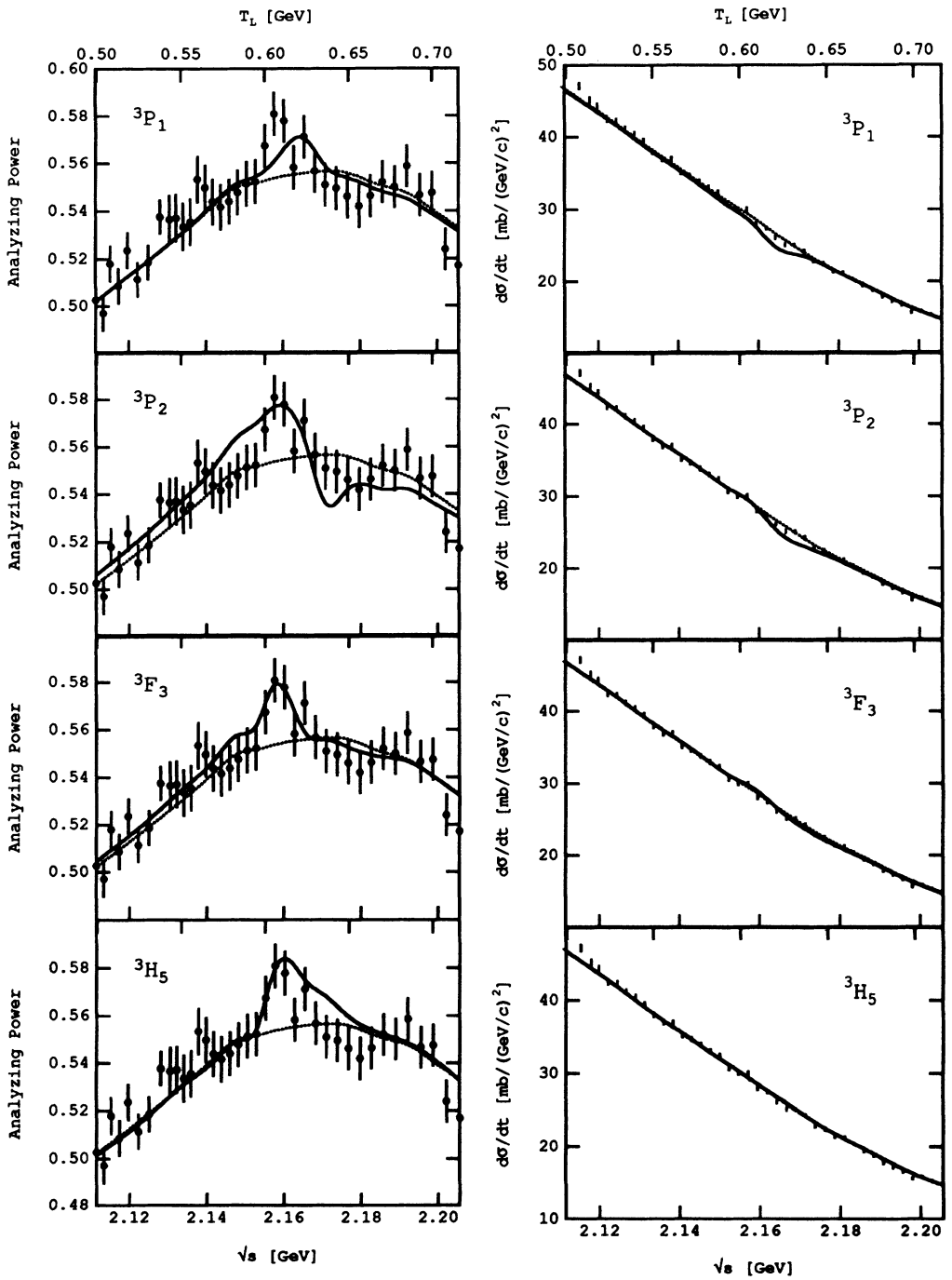

FIG. 2. The best-fit solutions of A_y and $d\sigma/d\Omega(\theta_c=90°)$ data with $^3P_1$, $^3P_2$, $^3F_3$, and $^3H_5$ resonances shown by the dotted lines. The solid lines are the corresponding backgrounds. Their resonance parameters are given in Table II.

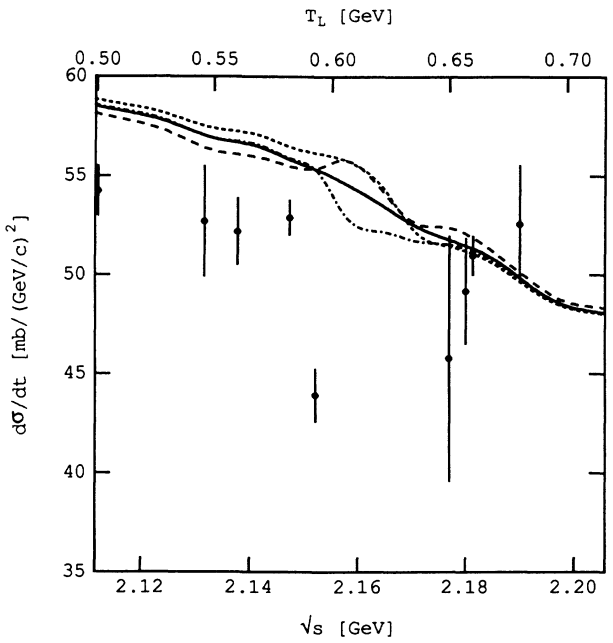

FIG. 3. The differential cross sections at the c.m.s. scattering angle $\theta_c = 40°$ in p-p scattering. The dashed, broken, and dot-dashed lines show the calculated values with $^3P_2$, $^3F_3$, and $^3H_5$ resonances, respectively, and the solid line shows their background. The experimental data at $\theta_c = 40°$ are given by several groups (see Table III).

onances, which are the most possible candidates for the origin of the narrow structure in the KEK A_y data in the p-p elastic scattering as discussed in Sec. III. The results are shown in Fig. 5. The structure parameters are the same as those given in Table II, and the elasticity is tentatively taken as $x = \Gamma_{\pi d}/\Gamma_t = 0.1$.

As is seen in this figure, the $^3d_3$ and $^3g_5$ cases give remarkably distinct effects to these experimental data at $\theta_c = 117°$ (see Table III). Therefore, the accurate measurement of $d\sigma/d\Omega$ and iT_{11} around $T_L = 170$ MeV and $\theta_c = 117°$ in the π-d elastic scattering could be useful for the discrimination between the $^3d_3$ and $^3g_5$ structures.

B. Analysis of $pp \to \pi d$ reaction

We also examine the effects of the narrow structures on the $pp \to \pi d$ reaction. The background amplitudes [$B_{J,J\pm1}$ in Eq. (2b)] are taken from Ref. [11]. The narrow structure term is defined by Eq. (4b):

$$R_{J,J-1} = \frac{1}{2}\sqrt{\eta_{pp}}\sqrt{\eta_{\pi d}}\, e^{i(\delta_{pp}+\delta_{\pi d})} \times \frac{\sqrt{\Gamma_{pp}}\sqrt{\Gamma_{\pi d}}}{-\sqrt{s}+\sqrt{s_R}-(i/2)\Gamma_t} c(\sqrt{s}) \,. \quad (4b)$$

Here η_{pp} ($\eta_{\pi d}$) and δ_{pp} ($\delta_{\pi d}$) are the phase-shifts and reflection parameters of elastic p-p (elastic π-d) scattering, respectively, for which we use the values obtained by the PSA mentioned above. The parameters of the narrow structure are the same as those in elastic p-p and π-d scattering.

We calculate the energy dependence of $d\sigma/d\Omega$ and A_{y0} at $\theta_c = 117°$ and 104° for $^3F_3$-$^3d_3$ and $^3H_5$-$^3g_5$ cases. The results are shown in Fig. 6.

As is seen from this figure, $^3F_3$-$^3d_3$ and $^3H_5$-$^3g_5$ structures give different effects to these experimental data (see Table III) similarly to the case in π-d elastic scattering. It is noted that the $^3H_5$-$^3g_5$ structure will be more preferable than the $^3F_3$-$^3d_3$ for the $d\sigma/d\Omega$ data at $\theta_c = 117°$

TABLE IV. The observables and their numbers of experimental data on elastic π-d scattering used in the PSA for determining the background term. The χ^2 values of the PSA solutions are also shown.

	Number of the used data						Total number	χ^2
T_L (MeV)	$d\sigma/dt$	iT_{11}	T_{20}	T_{20}^{lab}	τ_{22}	τ_{21}	of data[a]	value
65	21						21	26
80	9						9	10
117	18	10		1			29	43
125	20	16		1			37	40
134	31	22	6	7	6	12	84	110
140	105	17		18			140	224
151	21	11	6	1			39	37
180	41	21	4	4	6	10	86	142
189	22						22	27
219	34	17	6	2	6	12	77	104
238	17	13					30	41
256	86	39	12	4	6	6	153	226
275	18	16					34	31

[a]The data with $\chi^2 > 10$ have been excluded from the analysis and the χ^2 value.

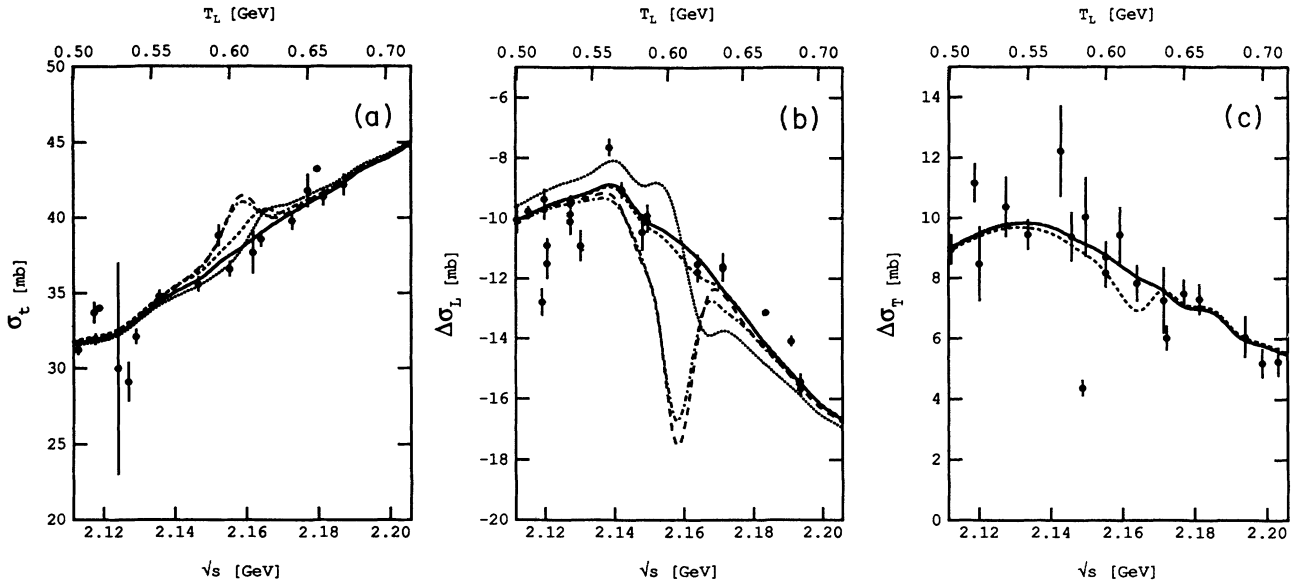

FIG. 4. The predicted values of forward observables σ_t^{pp}, $\Delta\sigma_L$, and $\Delta\sigma_T$, and their experimental data at present. The dotted, dashed, broken, and dot-dashed lines are the values of $^3P_1$, $^3P_2$, $^3F_3$, and $^3H_5$ resonances, respectively, and the solid lines their backgrounds.

and 104°, although the experimental errors [RI(70) and AL(71)] are large around $\sqrt{s}=2.15$–2.16 GeV. A_{y0} data at $\theta_c=104°$ measured by Yoshida [YO(91)] seem to have some structure around $\sqrt{s}=2.16$ GeV though old data do not, and this is consistent with the prediction of the $^3H_5$-$^3g_5$ structure. In order to obtain a more definite conclusion, one eagerly requires the measurements of this observable with high precision.

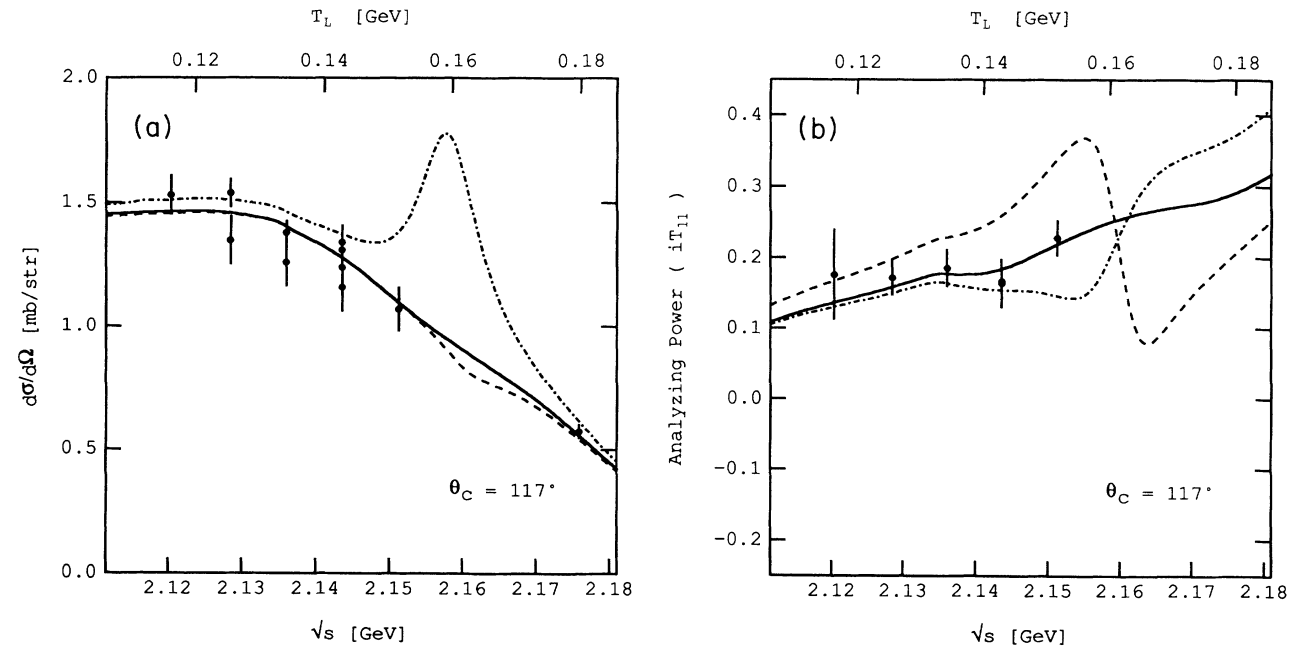

FIG. 5. (a) Experimental data on $d\sigma/d\Omega$ (see Table III) and the predicted values at $\theta_c=117°$ in π-d elastic scattering. The dashed and dot-dashed lines show the calculated values with admixture of $^3d_3$ and $^3g_5$ structure, respectively, while the solid line shows their background. The masses and total widths of the structures are the same as those given in Table II and elasticity $x=\Gamma_{\pi d}/\Gamma_t=0.1$. (b) Experimental data on the analyzing power (iT_{11}) (see Table III) and the predicted values at $\theta_c=117°$ in π-d elastic scattering. The curves have the same meaning as in (a).

V. CONCLUDING REMARKS

We have proposed a method of determining which spin parity of the partial wave generates the narrow structure in some observables. We utilize the interference term $b_{JP}(E,\theta)(\Gamma^i/[-\sqrt{s}+\sqrt{s_R}-(i/2)\Gamma_t])c(\sqrt{s})$ to find which partial wave is responsible for the structure, where b_{JP} is the structureless background. Using the b_{JP} which is usually known as being reliable, we find that the interference effect reflects on some observables a characteristic pattern depending on the b_{JP} term. By analyzing the pattern, we obtain information of which partial wave

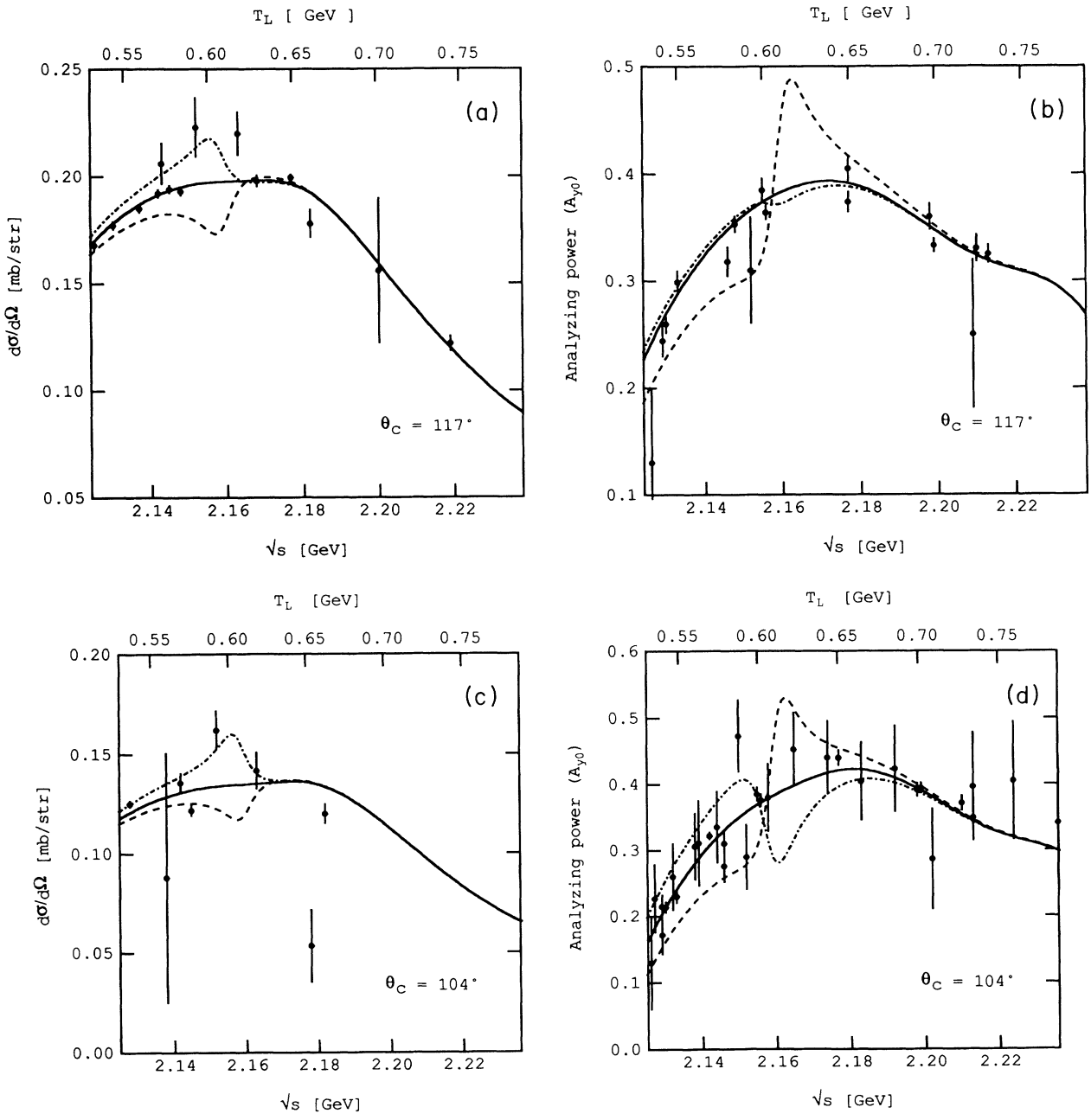

FIG. 6. (a) Experimental data on $d\sigma/d\Omega$ (see Table III) and the predicted values at $\theta_c=117°$ in pp-πd reaction. The dashed and dot-dashed lines show the calculated values with admixture of $^3F_3$-$^3d_3$ and $^3H_5$-$^3g_5$ structure, respectively, while the solid line shows their background. The masses, total widths, and elasticities Γ_{pp}/Γ_t are the same as those in Table II and $\Gamma_{\pi d}/\Gamma_t=0.1$. (b) Experimental data on A_{y0} (see Table III) and the predicted values at $\theta_c=117°$ in pp-πd reaction. The curves have the same meaning as in (a). (c) Experimental data on $d\sigma/d\Omega$ (see Table III) and the predicted values at $\theta_c=104°$ in pp-πd reaction. The curves have the same meaning as in (a). (d) Experimental data on A_{y0} (see Table III) and the predicted values at $\theta_c=104°$ in pp-πd reaction. The curves have the same meaning as in (a). (e) The data on A_{y0} [KEK YO(91)] at $\theta_c=104°$ in pp-πd reaction with the $^3H_5$ result (solid curve).

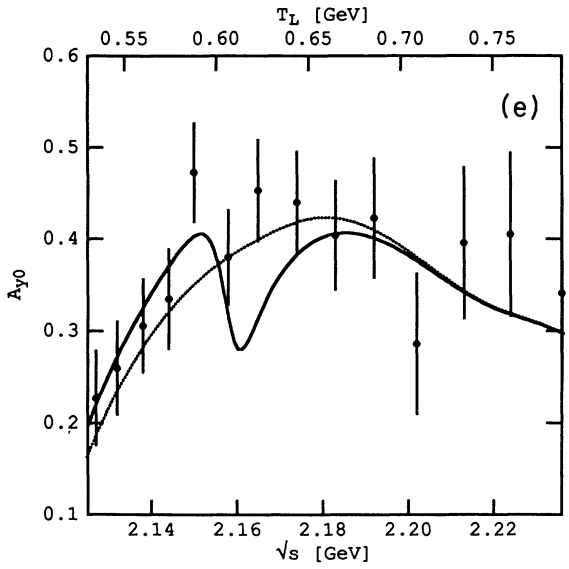

FIG. 6. (*Continued*).

generates the structure.

Applying this method to the analysis of the KEK A_y data and Saclay $d\sigma/d\Omega(\theta_c=90°)$ data at around $\sqrt{s}=2.16$ GeV, we find that the $^3F_3$ or $^3H_5$ wave is more favorable for the narrow structure than the others.

"Which of them could survive?" or "Is there any one that could survive?," however, is the next question. To answer this, more accurate data obtained at smaller energy intervals are needed.

The following observables are efficient in particular: σ_t^{pp}, $\Delta\sigma_L^{pp}$, $\Delta\sigma_T^{pp}$, and $d\sigma^{pp}/d\Omega$ ($\theta_c=40°$). We have shown how these data can select the correct solution from the two candidates.

The data on π-d scattering as well as *pp*-πd processes are also useful for this purpose. We have shown that $d\sigma/d\Omega$ and iT_{11} data on π-d scattering data at $\sqrt{s}\simeq 2.16$ GeV are relevant to discriminating the two candidates.

The data of $d\sigma/d\Omega$ and A_{y0} on *pp*-πd reaction are very useful as well. Especially, it is noted that, if only the $d\sigma/d\Omega$ data obtained RI(70) and AL(71) are used at $\sqrt{s}\approx 2.16$ GeV, the $^3H_5$ case is most suitable to describe the structure [see Fig. 6(a)]. Furthermore, the recent A_{y0} data measured at KEK [YO(91)] seem to have some structure at $\sqrt{s}\approx 2.16$ GeV, although the old data do not, and $^3H_5$ is consistent with the new data [see Fig. 6(e)]. However, there exist contradictory data obtained by other groups at the same energy [see Fig. 6(d)]. Then more accurate data at the same energy are required for this comparison.

The present result shows that each partial width for the *pp* and πd channels is compatible with about 10% of the total. Therefore unitarity requires that the rest of the 80% is shared by the πNN and $\pi\pi NN$ channels. Some remarkable effect would be seen in any of these channels.

We have parametrized the structure term by the resonance formula. This is only a conventional parametrization. While the present results seem to be consistent with the parametrization, we do not always claim that the structure is due to "some resonance." It seems that the narrow structure could represent a diproton. However, one should make a pole search on the complex energy plane before drawing this conclusion. At present the nature of the origin of the structure is very puzzling. It is especially noteworthy that the high-spin state like $J=3$ or 5 is in favor of the structure.

ACKNOWLEDGMENTS

The authors wish to thank Dr. H. Shimizu for useful discussions on the present problem and for communication about the experimental data. They greatly appreciate also Dr. M. Garçon for his careful reading of this manuscript.

[1] I. P. Auer *et al.*, Phys. Lett. **67B**, 113 (1977); I. P. Auer *et al.*, *ibid.* **70B**, 475 (1977); I. P. Auer *et al.*, Phys. Rev. Lett. **41**, 354 (1978).

[2] K. Hashimoto, Y. Higuchi, and N. Hoshizaki, Prog. Theor. Phys. **64**, 1678 (1980); M. Akemoto, M. Matsuda, H. Suemitsu, and M. Yonezawa, *ibid.* **67**, 554 (1982); R. A. Arndt, J. S. Hyslop III, and L. D. Roper, Phys. Rev. D **35**, 128 (1987).

[3] T. Ueda, Phys. Lett. **79B**, 487 (1978); Nucl. Phys. **A463**, 69c (1987).

[4] (a) B. Tatischeff *et al.*, Phys. Rev. Lett. **52**, 2022 (1984); Phys. Lett. **154B**, 107 (1985); (b) L. Santi *et al.*, Phys. Rev. C **38**, 2466 (1988).

[5] H. Shimizu *et al.*, KEK Report No. 89, 146 (1989); Phys. Rev. C **42**, R483 (1990); in Proceedings of the Xth International Seminar on High Energy Physics Problems—Dubna 1990; KEK Report No. 91-135, 1991.

[6] T. Ueda, Prog. Theor. Phys. **78**, 521 (1987).

[7] M. Garçon, D. Legrand, R. M. Lombard, B. Mayer, M. Rouger, Y. Terrien, and A. Nakach, Nucl. Phys. **A445**, 669 (1985).

[8] C. Fayard (private communication).

[9] N. Hiroshige, W. Watari, and M. Yonezawa, Prog. Theor. Phys. **84**, 941 (1990).

[10] N. R. Stevenson and Y. M. Shin, Phys. Rev. C **36**, 1221 (1987).

[11] N. Hiroshige, W. Watari, and M. Yonezawa, Prog. Theor. Phys. **72**, 1146 (1984).